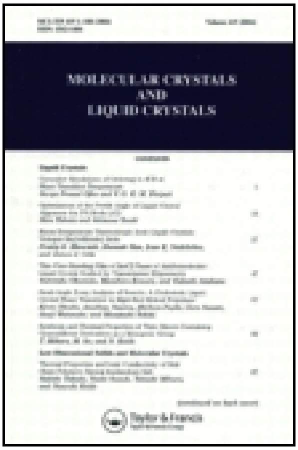

Molecular Crystals and Liquid Crystals

Publication details, including instructions for authors and subscription information:
http://www.tandfonline.com/loi/gmcl20

Modeling the Dynamics of Photo-induced Reorientation of Nematic Liquid Crystals doped with Azo-dye

David Statman [a] & James C. Lombardi Sr. [a]

[a] Allegheny College, Meadville, PA, USA

To cite this article: David Statman & James C. Lombardi Sr. (2008): Modeling the Dynamics of Photo-induced Reorientation of Nematic Liquid Crystals doped with Azo-dye, Molecular Crystals and Liquid Crystals, 494:1, 1-10

To link to this article: http://dx.doi.org/10.1080/15421400802429911

Mol. Cryst. Liq. Cryst., Vol. 494, pp. 1–10, 2008
Copyright © Taylor & Francis Group, LLC
ISSN: 1542-1406 print/1563-5287 online
DOI: 10.1080/15421400802429911

Modeling the Dynamics of Photo-induced Reorientation of Nematic Liquid Crystals doped with Azo-dye

David Statman and James C. Lombardi, Sr.
Allegheny College, Meadville, PA, USA

We have used a continuum model of azo-*dye doped liquid crystals to describe the dynamics of photo-induced enhancement of director re-orientation. By describing the dye distribution as a superposition of spherical harmonic functions we numerically integrate the dynamic equations and identify various time constants associated with* cis *to* trans *isomerization, excited state lifetime, and the various diffusion times of the different species. Our results give an experimental response time which is intensity dependent and characterized by a saturation intensity. This saturation intensity is dependent on the pump beams angle of incidence. Numerical results will be presented.*

Keywords: dyed nematics; modeling; photo-induced reorientation

1. INTRODUCTION

The effect of dyes on the photo-induced orientation or reorientation of liquid crystals has generated much interest and is well documented in the literature. First observed by Jánossy, Lloyd and Wherrett [1], it was found that small amounts of anthraquinone dye were capable of reducing the optical Freédericksz transition by more than two orders of magnitude. Further analysis demonstrated that this enhancement was the result of a photoinduced torque proportional to the optical torque:

$$\tau = (1+\eta)\langle \mathbf{P} \times \mathbf{E} \rangle \tag{1}$$

with η being the enhancement factor, and **P** and **E** are the polarization and electric field respectively. Since that time, many studies

Acknowledgement is made to the donors of The American Chemical Society Petroleum Research Fund for partial support of this research.

Address correspondence to David Statman, Allegheny College, 520 North Main Street, Meadville, PA 16335, USA. E-mail: david.statman@allegheny.edu

have been conducted with various dyes. It has been found that the enhancement factor is dye specific and can be either positive or negative, depending on whether the photoinduced torque is in the same or opposite direction as the optical torque. This dye induced enhancement, also referred to as the *Jánossy effect*, comes from a balance between the intermolecular forces and the diffusive forces between the dye, in its various states, and the liquid crystal host [2–6]. More recently, Truong, *et al.* [7] studied the dynamics of the interaction between the anthraquinone dye and the liquid crystal in the isotropic phase and report that rotational diffusion is decreased upon excitation of the dye. They note that the rotational diffusion coefficient can be approximated by an Arrhenius-type expression, in which the "activation" energy is determined by the guest host interaction.

Azo dyes provide an interesting twist to this photoinduced torque, as they can be found in the stable *trans* form or the meta-stable *cis* form. In the *trans* form, these dyes tend to exhibit a negative enhancement, while in the *cis* form they tend to exhibit a positive enhancement [8]. *Cis-trans* isomerization of the *azo* dyes may have an impact on the photoinduced torque not only because the structure, hence the molecular fields of the two isomers is different, but also because of the molecular motion involved in isomerization. Palffy-Muhoray and Weinan [9] have suggested that molecular motion induced by the light-induced *trans-cis* isomerization of *azo* dye dopants exerts the predominant influence in the observed enhancement effect, a phenomenon which they describe as an "orientational ratchet." In addition, the order parameter of the liquid crystal for two isomers is typically not the same [10], which may also impact the enhancement effect. Jánossy and Szabados [11,12] have proposed that the enhancement for *azo* dyes can be represented by the weighted sum of the individual enhancements of the two states, *cis* and *trans*. The relative strength of each state, *cis* or *trans*, is determined by the fraction of dye, X, in the *cis* state (the fraction in the *trans* state being $1–X$).

In this paper we present the results of numerical calculations examining the presence of three dye states, *trans*, *cis*, and excited, on the enhancement effect. The dye and nematic orientational distributions are represented by a superposition of spherical harmonic functions and applied to a simple diffusion model. In section 2, we present the model, based on diffusion equations. In section 3 we describe the results of our calculations. General conclusions are discussed in section 4.

2. THEORY

The dynamics of the liquid crystal host and the dye molecules in the *trans*, *cis*, and excited states are determined by rotational diffusion, rotational drift, photoexcitation, relaxation, and *cis* to *trans* isomerization. The equations describing these dynamics are given by the standard diffusion equation [2,5]

$$\frac{\partial f_\alpha}{\partial t} + \overline{\nabla} \cdot \mathbf{J}_\alpha = W_\alpha \qquad \alpha = h, t, c, e \tag{2}$$

where $\overline{\nabla}$ denotes the angular part of the standard differential operator ∇, the densities of the nematic host, and the *trans*, *cis* and excited state dye molecules are given by f_h,f_1,f_c, and f_e, respectively, and W_α are the transition rates between the different states of the dye molecules $W_h = 0$. The current densities, J_α, are described by rotational Brownian motion

$$\mathbf{J}_\alpha = -D_\alpha \overline{\nabla} f_\alpha - \frac{D_\alpha}{kT}(\overline{\nabla} U_\alpha) f_\alpha \tag{3}$$

where D_α are the rotational diffusion coefficients. The first term in Eq. (3) corresponds to rotational diffusion, whereas the second term corresponds to the rotational drift in the presence of a molecular field. This rotational drift is related to the torque on the director, $\tau = -\overline{\nabla} U_\alpha$. The potential energies, U_α, are the orientational potential energies of the different species. They consist of the mean-field effect of the intermolecular interactions, which are structure dependent. They also consist of the direct coupling to any external electromagnetic field to the liquid crystal.

In general, the solutions for the molecular densities, f_α, can be given by a superposition of spherical harmonic functions [13,14]

$$f_\alpha(\theta, \phi, t) = \frac{1}{4\pi} \sum_{l=0,2,4,\ldots} \sum_{m \le l} (2l+1) \left(\frac{l-|m|}{l+|m|} \right) Y_{l,m}(\theta, \phi) Q_i^{l,m}(t) \tag{4}$$

where $Q_\alpha^{l,m}$ are the moments of the distribution. The time dependence of the moments of the liquid crystal orientation distribution, $Q_h^{l,m}$, are given by [13]

$$\begin{aligned} Q_h^{l,m}(t) = Q_h^{l,m}(pure) + \frac{C_{l,m}}{\tau_{l,m}} \int_{-\infty}^{t} \Big[u_t Q_t^{l,m}(t') + u_c Q_c^{l,m}(t) + u_e Q_e^{l,m}(t) \Big] \\ \times e^{-} \big[(t-t')/\tau_{l,m} \big] dt' \end{aligned} \tag{5}$$

where $\tau_{l,m}$ is the relaxation time for mode *l,m*, $C_{l,m}$ is the strength of that mode, and $Q_h^{l,m}(pure)$ is the moment of the orientation for the un-doped liquid crystal. The steady state value for $Q_h^{2,1}$ determines the Jánossy effect enhancement factor, η, viz [13]:

$$\eta = \frac{Q_h^{2,1}[dyed]}{Q_h^{2,1}[pure]} \tag{6}$$

If the reorientation angle is in the *xz*-plane and is small, then the only terms of importance for this analysis are $Y_{0,0}, Y_{2,0}$, and $Y_{2,1}$. This expansion can thus be simplified as [14]:

$$f_i(\theta,\phi,t) = \frac{1}{4\pi}\left[N_i(t) + 5Q_i^{2,0}(t)P_2^0(\cos\theta) + \frac{5}{3}Q_i^{2,1}(t)P_2^1(\cos\theta)\cos\phi\right] \tag{7}$$

where the zeroth moments, N_i, correspond to the number density of each species $I, P_l^m(x)$ are the associated Legendre polynomials, and $Q_i^{2,1} = Q_i^{2,1}$. For simplicity, we eliminate the superscript 2 in the second moments: $Q_i^{2,0} \to Q_i^0$ and $Q_i^{2,1} \to Q_i^1$. For small reorientation angles, changes in the symmetric second moment $Q_i^{2,0}$ describe the change in the order of species *i*, hence impacting the liquid crystal order. The anti-symmetric second moment $Q_I^{2,1}$ corresponds to director reorientation [14]. This is visualized in Figs. 1a–d, where we show the contributions of the spherical harmonic functions to the orientational distribution.

Using the mean-field approximation, the potentials in Eq. (3) are given by the Maier-Saupe expression [15]:

$$U_i = -\frac{1}{3}u_i S_h P_2^0(\cos\theta) \tag{8}$$

where u_i is the orientational interaction energy between the liquid crystal and species *i* and S_h is the liquid crystal order parameter. The source-sink term, W_i, on the right hand side of Eq. (2) is given by [13]

$$W_t = -p_t(\cos\theta)f_t + \frac{F_t}{\tau_t}f_e + \frac{1-F_t}{\tau_t}\frac{N_e}{4\pi} + \frac{F_{c\to t}}{\tau_{c\to t}}f_c + \frac{1-F_{c\to t}}{\tau_{c\to t}}\frac{N_c}{4\pi}$$

$$W_c = -p_c(\cos\theta)f_c + \frac{F_c}{\tau_c}f_e + \frac{1-F_c}{\tau_c}\frac{N_e}{4\pi} - \frac{1}{\tau_{c\to t}}f_c$$

$$W_e = p_t(\cos\theta)f_t + p_c(\cos\theta)f_c - \left(\frac{1}{\tau_t} + \frac{1}{\tau_c}\right)f_e$$

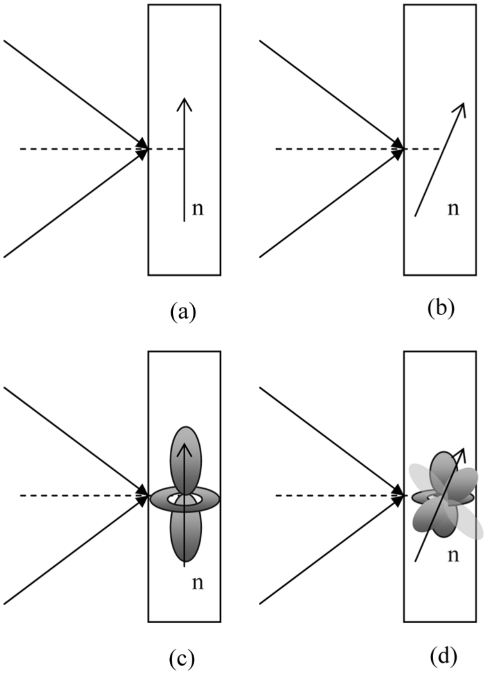

FIGURE 1 (a). Prior to reorientation, orientation distribution is symmetric around surface normal; (b) After reorientation, orientation is anti-symmetric around normal; (c) Only contribution to the orientational distribution of the liquid crystal is $Q_h^0 \cdot Q_h^1$ is zero; and (d) The second moment, Q_h^0, decreases. The second moment Q_h^1 becomes non-zero.

where [14]

$$p_i(x) = \frac{3\alpha_i}{h\nu N_D} I \left[P_2^0(x)\cos^2\Theta + \frac{2}{3}P_2^1(x)\cos\phi\sin\Theta\cos\Theta + \frac{1}{6}P_2^2(x)(1+\cos 2\phi\sin^2\Theta) \right],$$

α_i is the linear absorption coefficient, and N_D is the total number density of the dye, h is Planck's constant, and I and ν are the intensity and frequency of the incident light, respectively. The angle Θ is the angle the optical field makes with the z-axis. The constants F_t, F_c, and $F_{c \rightarrow t}$ correspond to the fraction of molecules preserving their orientation when relaxing from the excited state to the *trans* state, to the *cis* state, or from the *cis* state to the *trans* state, respectively [13]. These have the effect of increasing the relaxation times for those respective expressions.

3. RESULTS

We begin by substituting Eq. (7) into Eqs. (2) and (3) and solving for Q_h^1 at steady state *c.f.* Eq. (5). This is used to determine the enhancement factor, η, using Eq. (7). In doing so, we find that for times longer than the diffusion and electronic relaxation times, enhancement of photoinduced reorientation is characterized by the liquid crystal relaxation time and a second time related to the *cis* to *trans* isomerization time. The second time is determined by a saturation intensity;

$$\tau = \frac{\tau_{c\to t}}{1 + I/I_{sat}} \tag{9}$$

As suggested by Jánossy and Szabados [8], the enhancement factor itself can be separated into contributions from both the *trans* and *cis* states of the dye;

$$\eta = \eta_t(1 - X) + \eta_c X = \eta_t + X(\eta_c - \eta_t) \tag{10}$$

where the *trans* and *cis* enhancement factors are [14]

$$\begin{gathered}\eta_t \approx \frac{6}{5}\frac{\alpha_t}{h\nu}u_e\tau_{Qe}\left(\frac{cn_e\varepsilon_0}{\Delta\varepsilon N_h}\right)\left(\frac{21\alpha_c/\alpha_t}{21 - S_h u_t/kT}\right)\\ \left(1 - \frac{u_t\tau_{Qt}}{u_e\tau_{Qe}} + F_t\frac{u_t\tau_{Qt}}{u_e\tau_t} + F_c\frac{u_c\tau_{Qc}}{u_e\tau_c}\right)\end{gathered} \tag{11a}$$

$$\begin{gathered}\eta_c \approx \frac{6}{5}\frac{\alpha_t}{h\nu}u_e\tau_{Qe}\left(\frac{cn_e\varepsilon_0}{\Delta\varepsilon N_h}\right)\left(\frac{21\alpha_c/\alpha_t}{21 - S_h u_t/kT}\right)\\ \left(1 - \frac{u_c\tau_{Qc}}{u_e\tau_{Qe}} + F_t\frac{u_t\tau_{Qt}}{u_e\tau_t} + F_c\frac{u_c\tau_{Qc}}{u_e\tau_c}\right)\end{gathered} \tag{11b}$$

and S_h is the nematic order parameter. In Eqs. (11), the enhancement factors are primarily determined by the potentials u_t, u_c, and u_e, as well as the times $\tau_{Qt} \approx 1/6D_t$, $\tau_{Qt} \approx \frac{1}{6D_c + \frac{1}{\tau_{c\to t}}}$, and $\tau_{Qe} \approx \frac{1}{6D_e + \left(\frac{1}{\tau_t} + \frac{1}{\tau_c}\right)}$. The latter indicates that the more time the dye spends in a particular state, the more impact that state has on enhancement [14].

Equation (10) is consistent with previous work showing that the overall enhancement is determined by the fraction of dye in the *cis* state [8], $X = \frac{X_{sat}I/I_{sat}}{1+I/I_{sat}}$, where X_{sat} is the saturation fraction given by

$$X_{sat} = \frac{1}{1 + R\frac{\alpha_c\tau_c}{\alpha_t\tau_t}} \tag{12}$$

and I_{sat} is the same saturation intensity in Eq. (9), given by

$$I_{sat} = WX_{sat}\frac{N_D h\nu}{(\alpha_t\Phi_{tc}\tau_{c\to t})} \tag{13}$$

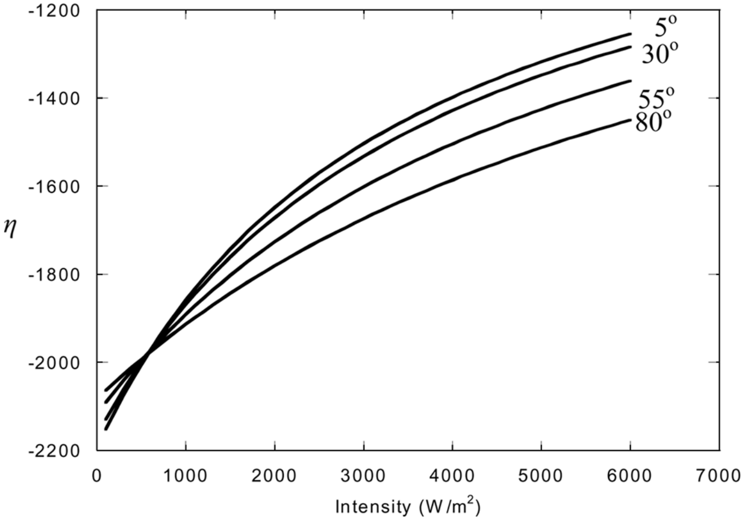

FIGURE 2 Calculated photoinduced enhancement versus intensity for four different incident angles.

Equations (12) and (13) differ from those previously derived [8] in that they include the factors R and W, respectively, given by

$$R = \frac{u_c}{u_t}\left(\frac{21 - S_h u_t/kT}{21 - S_h u_c/kT}\right) \tag{14}$$

and

$$W = \left(\frac{5}{7}\right)\left(\frac{21 - S_h u_t/kT}{U_t/kT}\right)\left(\frac{1}{3\cos^2\Theta - 1}\right) \tag{15}$$

These factors indicate that both the saturation fraction and the saturation intensity are determined by the dye's environment and the saturation intensity is also determined by the pump angle of incidence.

These analytic results are supported by numerical calculations. Steady state calculations of the enhancement factor for four external pump anlges are shown in Figure 2. These calculations were fit to Eq. (10). The results of that fit are shown in Table 1. As can be seen, the enhancement factors are relatively insensitive to the pump angle of incidence. The saturation intensity, on the other hand, clearly increases with pump angle, as expected from Eq. (13). In fact, the fit values for the saturation intensity agree exactly with those calculated from Eq. (13).

TABLE 1 Determination of enhancement factor and saturation intensity from fits to numerical calculation

Angle	5°	30°	55°	80°
η_t	−2194	−2166	−2118	−2083
η_c	255	252	246	242
$I_{sat}(W/mm^2)$	3383	3861	5241	7228

In Figure 3, we show the calculated time dependence of the enhancement factor for two pump intensities at the same pump angle. In these calculations, we chose a very fast nematic reorientation time so that we might only consider the effect of the dye. These calculations fit very well to a single exponential for times longer than a few milliseconds. This indicates that *cis* to *trans* isomerization dominates the dynamics of the photoinduced enhancement. This, of course, is expected, as the *cis* to *trans* isomerization time is much longer than the diffusion times and the excited state lifetimes. When the fit single exponential is extrapolated back to $t = 0$, the intercept is given by η_t.

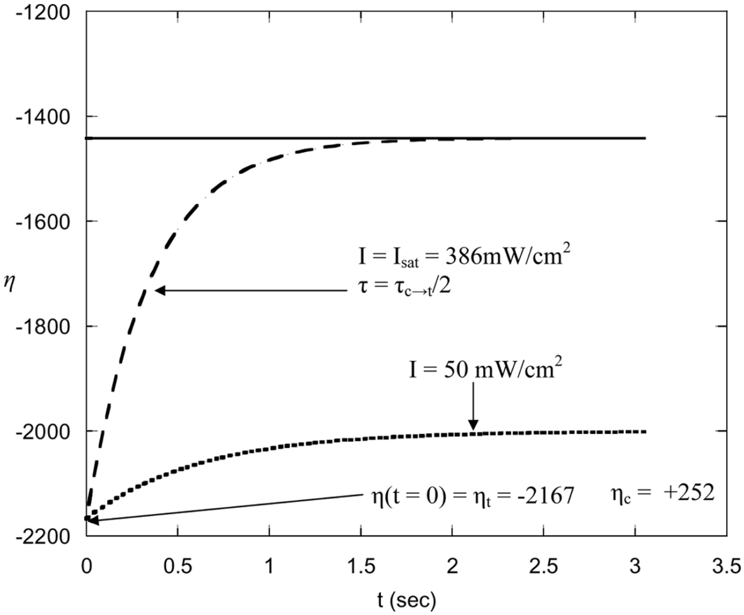

FIGURE 3 Photoinduced enhancement versus time for two pump intensities. The nematic reorientation time is much faster than the dye relaxation time.

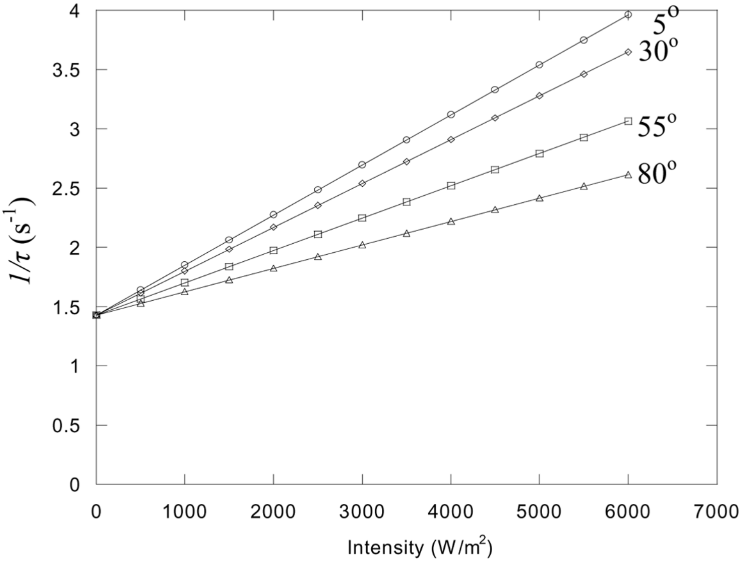

FIGURE 4 Calculated time constants, $1/\tau$, versus intensity.

Again, this should not be surprising, since this is prior to the formation of *cis* isomers. These extrapolated values for the enhancement factor at $t = 0$ agree with those determined from steady state values.

The single exponential fits of the enhancement factor to time also show that the time constant is intensity dependent, and determined by the saturation intensity. This is shown for four external pump angles in Figure 4. At each pump angle, the inverse of the response time is linear with intensity. These calculations agree with Eq. (9), with the intercept being given by the inverse of the *cis* to *trans* isomerization time, and the intercept divided by the slope being given the saturation intensity.

5. CONCLUSIONS

In this paper, we have compared numerical calculations of photoinduced reorientation with analytic solutions based on some approximation. Our results demonstrate that the saturation intensity and saturation fraction of the dye is dependent on the liquid crystal environment, while the saturation intensity is also dependent on the incident angle of the pump beam. These results also suggest that dynamic studies of photoinduced reorientation provide an alternative method of determining the *cis* to *trans* isomerization time of the *azo* dye in the nematic, as well as the angular dependent saturation intensity. In these calculations, it is assumed that the nematic response time is very fast. In most experimental systems, this would not be the case. In previous experimental studies [14], we examined the dynamics of photoinduced reorientation by measuring how the birefringence of the liquid crystal changed in time. We found those dynamics to be characterized by a triple exponential with an additional long tail. It is likely that the long tail is the result of gliding of the director at the surface. It is also possible that the third exponential is due to thermal effects altering the birefringence of the liquid crystal. Of the remaining exponentials, we expect one to be associated with the nematic relaxation time, and the other to be associated with the *cis* to *trans* isomerization time. In the future, we plan to identify that contribution associated with *cis* to *trans* isomerization, and compare it with model calculations.

REFERENCES

[1] Jánossy, I., Lloyd, A. D., & Wherrett, B. S. (1990). *Mol. Cryst. Liq. Cryst.*, *179*, 1.

[2] Jánossy, I. (1994). *Phys. Rev. E*, *49*, 2957.

[3] Marrucci, L. & Paparo, D. (1997). *Phys. Rev. E*, *56*, 1765.

[4] Marrucci, L., Paparo, D., Abbate, G., Santamato, E., Kreuzer, M., Lehnert, P., & Vogeler, T. (1998). *Phys. Rev. A*, *58*, 4926.

[5] Paparo, D., Marrucci, L., Abbate, G., Santamato, E., Kreuzer, M., Lehnert, P., & Vogeler, T. (1997). *Phys. Rev. Lett.*, *78*, 38–41.

[6] Marrucci, L., Paparo, D., Maddalena, P., Massera, E., Prudnikova, E., & Santamato, E. (1997). *J. Chem. Phys.*, *107*, 9783–9792.

[7] Truong, T. V., Xu, L., & Shen, Y. R. (2005). *Phys. Rev. E*, *72*, 051709.

[8] Jánossy, I. & Szabados, L. (1998). *Phys. Rev. E*, *58*, 4598–4604.

[9] Palffy-Muhoray, P. & Weinan, E. (1998). *Mol. Cryst. Liq. Cryst.*, *320*, 193–206.

[10] Mustroph, H. & Epperlein, J. (1981). *J. Prakt. Chem.*, *323*, 755–775.

[11] Jánossy, I. & Szabados, L. (1998). *J. Nonlin. Opt. Phys. Mat.*, *7*, 539.

[12] Jánossy, I. & Szabados, L. (1998). *Phys. Rev. E*, *58*, 4598.

[13] Truong, T. V., Xu, L., & Shen, Y. R. (2005). *Phys. Rev. E*, *72*, 051709.

[14] Statman, D., Page, E., Werner, V., & Lombardi, J. C. (2007). *Phys. Rev. E.*, *75*, 021703.

[15] DeGennes, P. G. & Prost, J. (1993). *The Physics of Liquid Crystals*, 2nd Ed. Oxford Science, p. 66.